JOURNAL OF Applied Polymer SCIENCE

Assessment of Cell Proliferation in Salt-Leaching Using Powder (SLUP) Scaffolds with Penetrated Macro-Pores

Yong Sang Cho,[1] Myoung Wha Hong,[2] Young Yul Kim,[2] Young-Sam Cho[1]

[1]Division of Mechanical and Automotive Engineering, College of Engineering, Wonkwang University, Iksan, Jeonbuk 570-749, Republic of Korea

[2]Daejeon St. Mary's Hospital, Catholic University of Korea, Republic of Korea

Correspondence to: Y.-S. Cho (E-mail: youngsamcho@wku.ac.kr) or Y. Y. Kim (E-mail: kimtwins72@hanmail.net)

ABSTRACT: In this study, a salt-leaching using powder (SLUP) scaffold with penetrated macropores was proposed to enhance cell proliferation. A SLUP scaffold is a salt-leaching scaffold with an arbitrary pore configuration. Although SLUP scaffolds have several advantage over traditional salt-leaching scaffolds, the cell ingrowth might be poor compared with solid freeform fabrication scaffolds, which have well-interconnected pores. We therefore proposed SLUP scaffolds with penetrated macropores to assist the cell ingrowth. First, polycaprolactone (PCL) powders with a grain size of 63–100 μm and NaCl powders with a grain size of 100–180 μm were prepared. Next, a uniformly perforated mold was fabricated using an rapid prototyping (RP) system. Then, 500-, 820-, or 1200-μm-diameter needles were inserted into the holes of the RP mold. Subsequently, the mold was filled with a mixed powder of PCL/NaCl (30 : 70 vol %). The mold was then heated in the oven at 100°C for 30 min, and both the needles and the mold were removed from the PCL/NaCl mixture. Then, the PCL/NaCl mixture was soaked in DI water for 24 h to leach out NaCl particles and dried in a vacuum desiccator for 24 h. The porosity of fabricated scaffolds was calculated using a simple equation, and the compressive stiffness was measured using a universal testing machine. Moreover, each scaffold ($10 \times 10 \times 10$ mm^3) was seeded with 100,000 Saos-2 cells and cultured for 14 days. The cell proliferation characteristics were assessed using a CCK-8 assay at 1, 7, and 14 days for comparison with the control scaffolds, that is, the SLUP scaffolds with no penetrated macropores. © 2013 Wiley Periodicals, Inc. J. Appl. Polym. Sci. **2014**, *131*, 40240.

KEYWORDS: biomedical applications; manufacturing; porous materials

Received 15 August 2013; accepted 27 November 2013

DOI: 10.1002/app.40240

INTRODUCTION

Recently, tissue engineering has received attention as a potential approach to repairing damaged tissue. In tissue engineering, a scaffold is a key item that includes cells and a dynamic environment.[1–3] Because of the importance of scaffolds in tissue engineering, several traditional methods and solid freeform fabrication (SFF) methods have been developed. The representative traditional methods can be summarized as follows: salt-leaching,[4–10] phase separation,[11] gas-foaming,[12] and freeze-drying.[13] SFF methods can be classified as stereo lithography apparatus[14], selective laser sintering,[15] and three-dimensional (3D) printing.[16] Generally, SFF techniques can fabricate a scaffold with a well-defined geometry and well-interconnected pores. However, from the viewpoint of easiness and cost-effectiveness, the salt-leaching method, which is the representative of traditional methods, has some advantages.

Theoretically, a scaffold should have an appropriate 3D configuration suitable for tissue regeneration. Moreover, it needs well-interconnected pores to promote cell proliferation and differentiation.[17] For good cell proliferation and differentiation, a sufficient supply of oxygen is essential as well as the exchange of nutrients and waste is necessary. Additionally, space for cell proliferation should be provided in the scaffold. Therefore, several studies[18,19] have mentioned that both global and local pores should be offered in the scaffold to drive cell proliferation. To meet these requirements, the salt-leaching method is limited due to its resulting bad pore interconnections.

In this study, a salt-leaching using powder (SLUP) scaffold with penetrated macropores was proposed to enhance cell proliferation. The SLUP technique, which was proposed in a previous study[20] by our group, has several advantages compared to traditional salt-leaching scaffolds: it is a solvent-free and pressure-free technique. To fabricate SLUP scaffolds with penetrated macropores, which are global pores, polycaprolactone (PCL) powders with a 63–100 μm grain size and NaCl powders with a

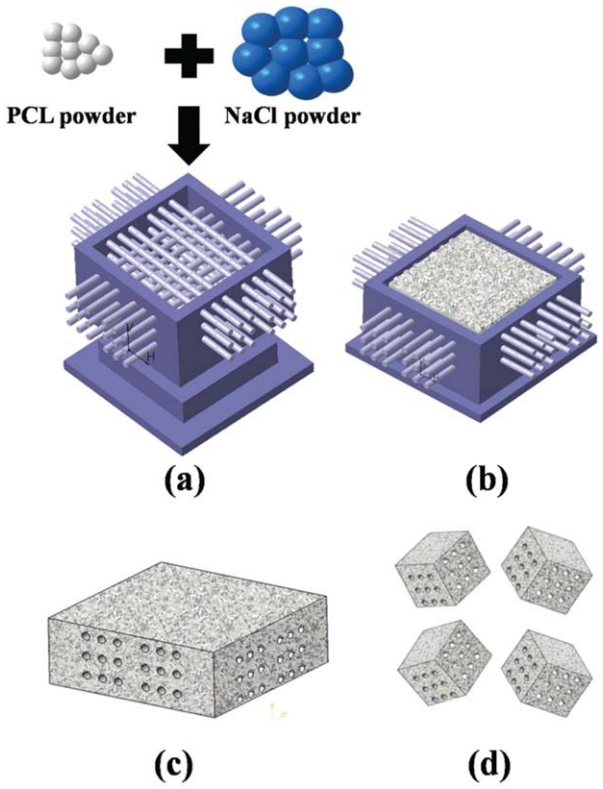

Figure 1. Fabrication procedure of a scaffold with global pores using the SLUP technique: (a) the PCL/NaCl (30 : 70 vol %) mixture was prepared, and needles with 500-, 820-, and 1200-μm diameters, respectively, were inserted into the holes in the uniformly perforated mold (with an inside dimension of $20 \times 20 \times 15$ mm^3); (b) the bottom cover (with a dimension of $20 \times 20 \times 5$ mm^3) was assembled, and the assembled mold was filled up with the mixture (PCL : NaCl = 30 : 70 vol %); (c) the SUS needles were removed, and the PCL/NaCl mixture was separated from the RP mold; and (d) the PCL/NaCl mixture was cut into cubes with volumes of $10 \times 10 \times 10$ mm^3. To leach out the NaCl, the scaffolds were soaked in a beaker filled with DI water for 24 h using a sonicator and dried for 24 h using a desiccator. [Color figure can be viewed in the online issue, which is available at wileyonlinelibrary.com.]

100–180 μm grain size were first prepared. Next, a uniformly perforated mold was fabricated using a rapid prototyping (RP) system. Subsequently, 500-, 820-, or 1200-μm-diameter needles were inserted into the holes of the RP mold, and the mold was filled with mixed powders of PCL/NaCl (30 : 70 vol %). Then, the mold was heated in the oven at 100°C for 30 min. Thereafter, the needles and the mold were removed from the PCL/NaCl mixture. The PCL/NaCl mixture was then soaked in DI water to leach out the NaCl particles for 24 h and dried in a vacuum desiccator for 24 h. Consequently, the remaining PCL structure had global pores (made by the needles) and local pores (made by the NaCl particles). To analyze the compressive modulus of the fabricated scaffold, a uniaxial compression test was performed using a universal testing machine (UTM), and the surface characteristic of the scaffold was observed using a scanning electron microscope (SEM). Additionally, cell-culture experiments were performed using Saos-2 cells, and the cell-proliferation characteristics were assessed via a CCK-8 assay with SLUP scaffolds without global pores as controls.

EXPERIMENTAL

Materials

PCL (M_n = 70,000–90,000, Sigma-Aldrich, MO), stainless steel needles (Dongbang Acupuncture, Korea), sodium chloride (Sigma-Aldrich), and sieves (DAIHAN Scientific, Korea) were purchased to fabricate the scaffold. Molds were designed using CATIA V5R13 and fabricated using the RP system (Eden 250, Stratasys, MN). Additionally, Saos-2 cells were obtained from the American type culture collection for cell-culture.

Mold Design

Three types of mold with holes of different sizes were designed and fabricated. Each mold had an outer dimension of $26 \times 26 \times 15$ mm^3 and an inner dimension of $20 \times 20 \times 15$ mm^3. To prevent pour-down of the powder mixture, the bottom covers were fabricated with a size of $20 \times 20 \times 5$ mm^3, as depicted in Figure 1(a). Consequently, each assembled mold had an inner dimension of $20 \times 20 \times 10$ mm^3. To insert the needles, each mold was designed to have 520, 840, or 1220-μm-diameter holes. The diameters of the needles used were 500, 820, and 1200 μm, respectively. In each assembly, each hole was fabricated with a tolerance of 20 μm. After that, the designed molds were fabricated using a RP system (Eden 250, Stratasys).

Fabrication of the Scaffolds

First, to obtain PCL powder with a grain size of 63–100 μm and NaCl powder with a grain size of 100–180 μm, PCL and NaCl were pulverized using a laboratory-made freeze grinder. Then, the PCL and NaCl powders were sieved using sieves of relevant mesh size. After that, mixtures of PCL/NaCl were prepared with a mixed volume ratio of 30 : 70 (PCL : NaCl). The reason of the chosen mixed volume ratio (30 : 70 [PCL : NaCl]) is the continuity from our previous study.[20] In our previous study, the chosen mixed volume ratio of 30 : 70 (PCL : NaCl) is the best result in our cell-proliferation experiments. Therefore, in this study, we tried to test the effect of global pores at the best condition of SLUP scaffold with continuous manner from our previous study. Second, the 500-, 820-, or 1200-μm-diameter needles were inserted into the holes in the uniformly perforated mold (with an inside dimension of $20 \times 20 \times 15$ mm^3) as shown in Figure 1(a). Subsequently, the bottom cover (with an inside dimension of $20 \times 20 \times 5$ mm^3) was assembled into the mold, and the mixture of PCL/NaCl particles was filled up into the mold, as shown in Figure 1(b). Afterward, the mold was heated in an oven at 100°C for 30 min. Subsequently, the steel use stainless (SUS) needles were removed, and the mixture of PCL/NaCl was separated from the RP mold, as depicted in Figure 1(c). Last, the mixture of PCL/NaCl was cut into cubes with dimensions of $10 \times 10 \times 10$ mm^3, as depicted in Figure 1(d), and the cut scaffolds were soaked in a beaker filled with DI water. Leaching out NaCl was performed for 24 h using a sonicator (the water was changed every 6 h)[6, 21–26], and then, the scaffolds were dried for 24 h using a desiccator. Consequently, the fabricated scaffolds were depicted in Figure 2. To evaluate the present scaffold, SLUP scaffolds without global pores [Figure 2(a)] were used as control scaffolds. The volume ratio of PCL to NaCl for the control group was 30 : 70. Three types of scaffold with different holes

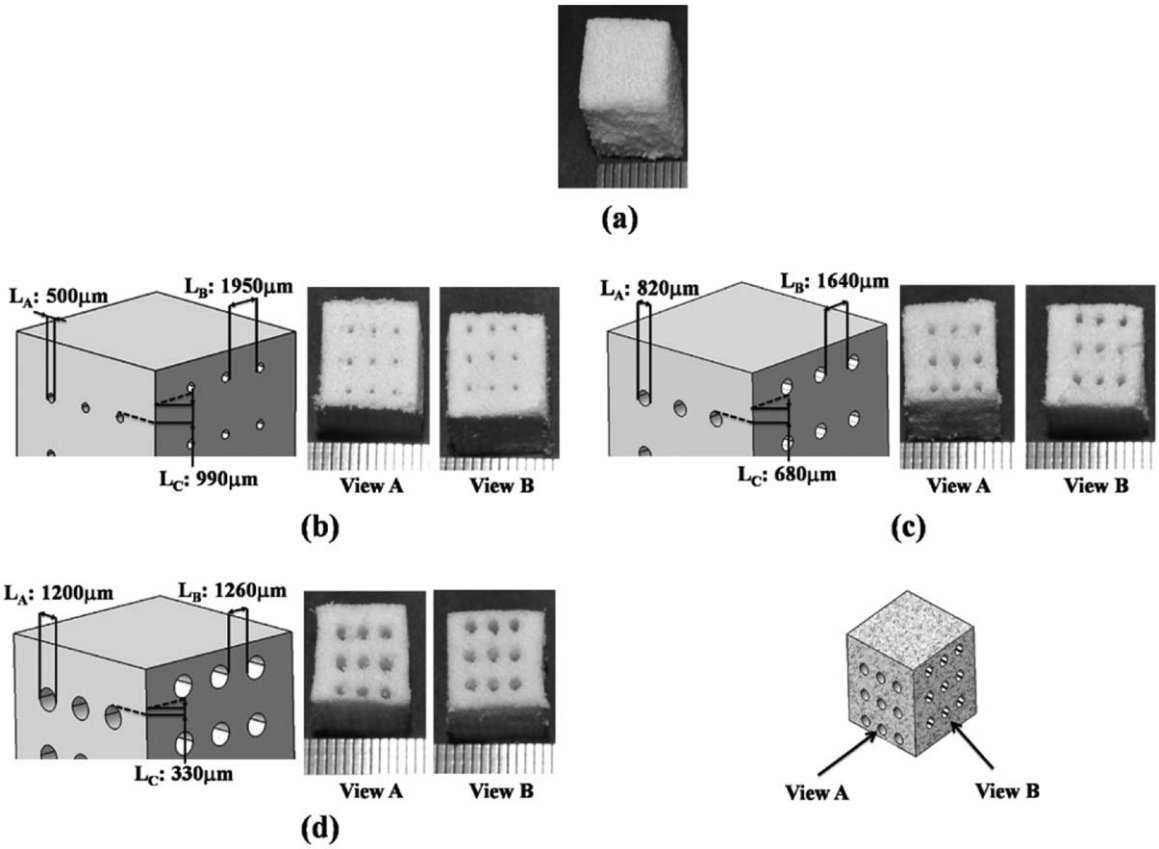

Figure 2. Images of fabricated scaffolds: (a) a fabricated control scaffold (PCL : NaCl = 30 : 70 vol %) without global pores; (b) a fabricated scaffold (PCL : NaCl = 30 : 70 vol %) with global pores (L_A=500 μm), the interval between unidirectional holes (L_B=1950 μm), and the interval between multidirectional global pores (L_C=990 μm); (c) a fabricated scaffold (PCL : NaCl = 30 : 70 vol %) with global pores (L_A=820 μm) with L_B=1640 μm and L_C= 680 μm; and (d) a fabricated scaffold (PCL : NaCl = 30 : 70 vol %) with global pores (L_A=1200 μm) with L_B=1260 μm and L_C= 330 μm.

were depicted in Figure 2(b–d). The diameter of the hole (L_A), the interval between unidirectional holes (L_B), and the interval between multidirectional global pores (L_C) are shown in Figure 2(b–d), respectively. 22 scaffolds were fabricated for each type of scaffold: 12 scaffolds were used for the cell assay and 10 scaffolds were used for the porosity calculation and the UTM test.

Cell Proliferation and CCK-8 Assays

After a few passages, cultured Saos-2 cells were detached using trypsin/EDTA [0.05% (w/v) trypsin, 0.02% (w/v) ethylenediaminetetraacetic acid, EDTA] (Gibco BRL). The scaffolds were sterilized by 70% ethyl alcohol overnight under UV light and then washed three times using phosphate-buffered saline (Hyclone). Saos-2 cells were seeded onto scaffolds at a concentration of 1×10^5 cells/10 μL Dulbecco's modified eagle's medium (DMEM) (Hyclone) and incubated for 30 min to allow the cells to attach to the scaffolds. After 30 min, the medium was added, and the cells were maintained in DMEM supplemented with 10% fetal bovine serum (Gibco BRL), 100 U/mL penicillin (Gibco BRL), and 100 μg/mL streptomycin (Gibco BRL). Culture was maintained at 37°C in a humidified incubator supplemented with 5% CO_2. Half of the media was changed every 3 days. Analytical assays were performed at 1, 7, and 14 days. Four specimens were used for each assay. Viable cells were measured using the Cell Counting Kit-8 (CCK-8, Dojindo, Japan), following the manufacturer's instructions. The cell proliferation was presented by the mean optical density value from three walls.

Statistical Analysis

All data are presented as means ± standard deviation. Statistical analyses, which is single-factor analyses of variance (ANOVA), were performed using SPSS version 21.0 software (SPSS, Chicago, IL). A value of $P < 0.05$ was considered statistically significant.

RESULTS AND DISCUSSION

Surface Structure Analysis of the Scaffolds

Using SEM (JSM-5410, JEOL, Japan) equipment, surface morphology and interconnectivity of fabricated scaffolds are observed. Figure 3(a,b) show surface and cross-section images, of a control scaffold without global pores, respectively. Additionally, Figure 3(c,e,g) show surface images of fabricated dual-pore scaffolds made with 500-, 820-, or 1200-μm-diameter needles, respectively. Figure 3(d,f,h) show cross-section images of dual-pore scaffolds fabricated with 500-, 820-, or 1200-μm-diameter needles, respectively. According to the SEM images, scaffolds that were proposed in this study seem to be dual-pore scaffolds, which have both global and local pores. Global pores were made with needles (500-, 820-, and 1200 μm in diameter),

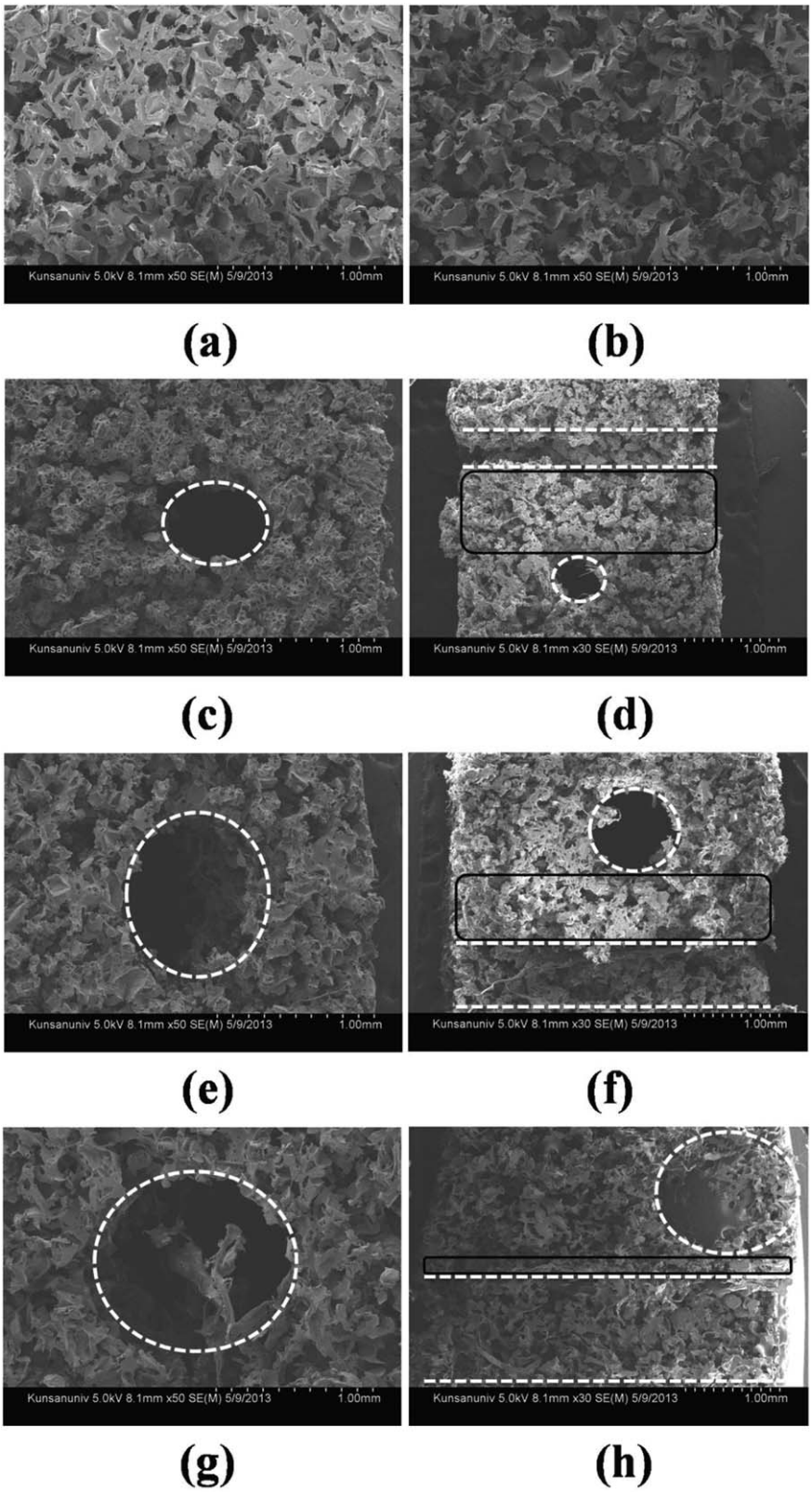

Figure 3. SEM images of fabricated scaffolds: (a) surface image, (b) cross-section image of a control scaffold, (c) surface image, and (d) cross-section image of a dual-pore scaffold with global pores (500 μm); (d) surface image and (e) cross-section image of a dual-pore scaffold with global pores (820 μm); (f) surface image and (g) cross-section image of a dual-pore scaffold with global pores (1200 μm) (white-dashed boxes: global pores generated by SUS needles, black solid box: region between multidirectional global pores).

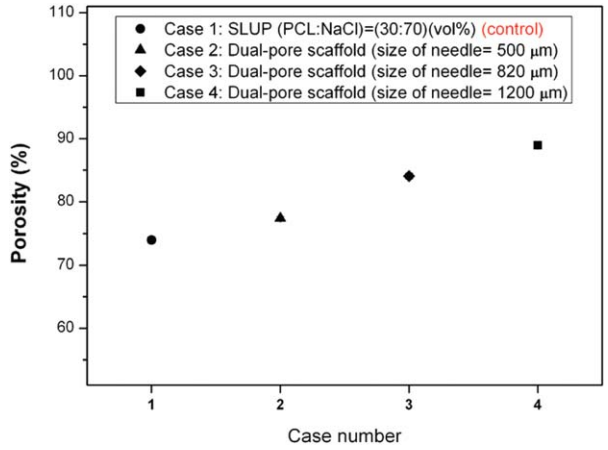

Figure 4. Calculated porosities of fabricated scaffolds with global pores and without global pores (control scaffold). [Color figure can be viewed in the online issue, which is available at wileyonlinelibrary.com.]

and local pores were formed by NaCl particles (100–180 μm). Especially, as depicted in Figure 3(d,f,h), the white dashed boxes mean fabricated global pores by needles (500, 820, and 1200 μm in diameter). Additionally, the black solid boxes indicate the space between different directional global pores. The region of the black box was decreased as the size of the needle was increased, as shown in Figure 3(d,f,h). As depicted in Figure 2, the interval between unidirectional global pores is also decreased (although it is not depicted in the SEM images) as the needle diameter increased, along with the interval between different directional global pores. Certainly, the larger global pores could provide more nutrients and oxygen. Additionally, relevant smaller regions between global pores [black solid box in Figure 3(d,f,h)] could make cell ingrowth easier.

Porosity Calculation

In cell scaffolds, porosity is an important parameter because the porosity indicates the total space proportion in the scaffold for cell proliferation. In this study, the porosity of the fabricated scaffold was calculated using eq. (1). For each type of scaffold, 10 scaffolds were used for the following calculation:

$$\text{porosity} = \frac{V_0 - \left({}^{m}/_{\rho}\right)}{V_0} \times 100(\%) \quad (1)$$

where V_0 is the apparent volume of the scaffold, which is calculated using the outer dimension of the scaffold, m is the mass of the scaffold without NaCl, and ρ is the density of the PCL.

As depicted in Figure 4, the porosity of the control scaffolds using SLUP with a volume ratio of 30 : 70 (PCL : NaCl) was calculated as $74.01 \pm 0.52\%$. The slightly larger porosity compared with the used volume ratio of PCL/NaCl is the characteristic of the SLUP technique due to the lack of pressure in the procedure. The porosities of the dual-pore scaffolds made by 500-, 820-, or 1200-μm-diameter needles were calculated as 77.37 ± 0.30, 84.09 ± 0.46, and $88.95 \pm 0.45\%$, respectively. As shown in Figure 4, the porosities of dual-pore scaffolds (using 500-, 820-, or 1200-μm-diameter needles) were greater than the porosity of the control scaffolds [SLUP with a volume ratio of 30 : 70 (PCL : NaCl)] because the dual-pore scaffolds have global pores made by needles.

Evaluation of Compressive Stiffness

To measure the compressive stiffness of the proposed scaffolds, a uniaxial compression test was performed using a UTM (Z020, Zwick/Roell) and 10 scaffolds for each scaffold type. As shown in Figure 5, the compressive stiffness of the dual-pore scaffolds, made with 500-, 820-, or 1200-μm-diameter needles, were measured as 0.862 ± 0.319, 0.710 ± 0.325, and 0.695 ± 0.223 MPa, respectively. In contrast, the control scaffolds were measured as 0.875 ± 0.215 MPa. In particular, as depicted in Figure 5, the compressive stiffness of the dual-pore scaffolds, made with 500-μm-diameter needles, and the control scaffolds were nearly identical. Additionally, compressive stiffness of the dual-pore scaffolds made with 820-μm-diameter needles was similar to the compressive stiffness of the dual-pore scaffolds made with 1200-μm-diameter needles. As a result, compressive stiffness of the dual-pore scaffolds made with 820- or 1200-μm-

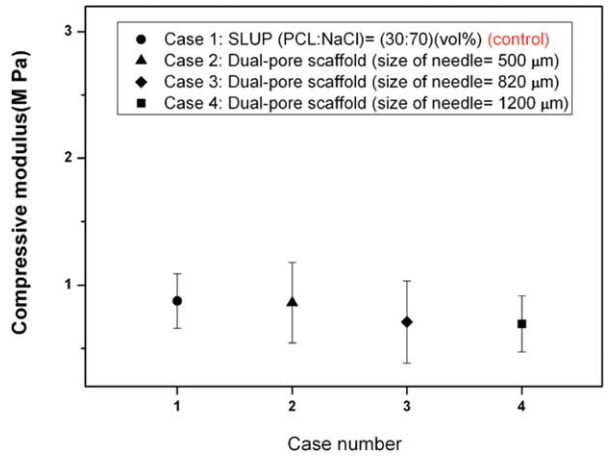

Figure 5. Compressive moduli of fabricated scaffolds with global pores and without global pores (control scaffold). [Color figure can be viewed in the online issue, which is available at wileyonlinelibrary.com.]

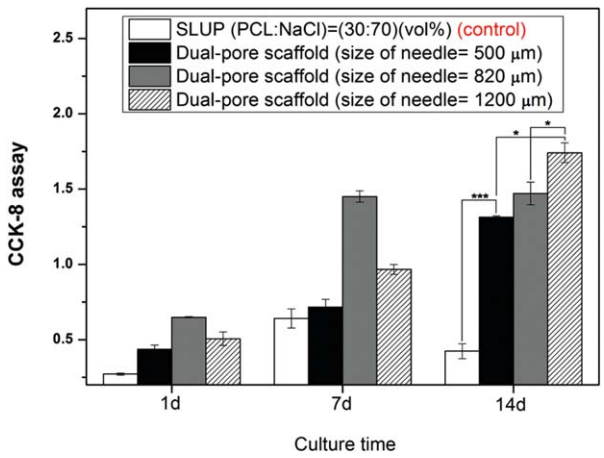

Figure 6. CCK-8 assay results of cell proliferation on fabricated scaffolds at 1, 7, and 14 days ($^{*}P < 0.05$, $^{***}P < 0.001$). [Color figure can be viewed in the online issue, which is available at wileyonlinelibrary.com.]

Table I. Apparent Surface Area Change of Scaffold Types

Scaffold types	Apparent surface area, $A_O + A_I$ (mm^2)	Apparent outer surface area, A_O (mm^2)	Apparent inner surface area generated by needles, A_I (mm^2)
Control scaffold	600	600	NA
Dual-pore scaffold (with 500-μm global pores)	876	593	283
Dual-pore scaffold (with 820-μm global pores)	1045	581	464
Dual-pore scaffold (with 1200-μm global pores)	1238	559	679

diameter needles was smaller than that of the control scaffolds by approximately 20%. It could not be negligible values in the manner of relative values. As shown in Figure 5, the compressive moduli of fabricated SLUP scaffolds are very low (<1 MPa). Therefore, the applicable tissue of the proposed scaffolds should be almost payload-free or force-free. At least, the payload or external force at the applicable tissue should be controllable.

Analysis of Cell-Culture Characteristics

The cell-culture characteristics of the fabricated scaffolds were observed using CCK-8 assays for 1, 7, and 14 days. As shown in

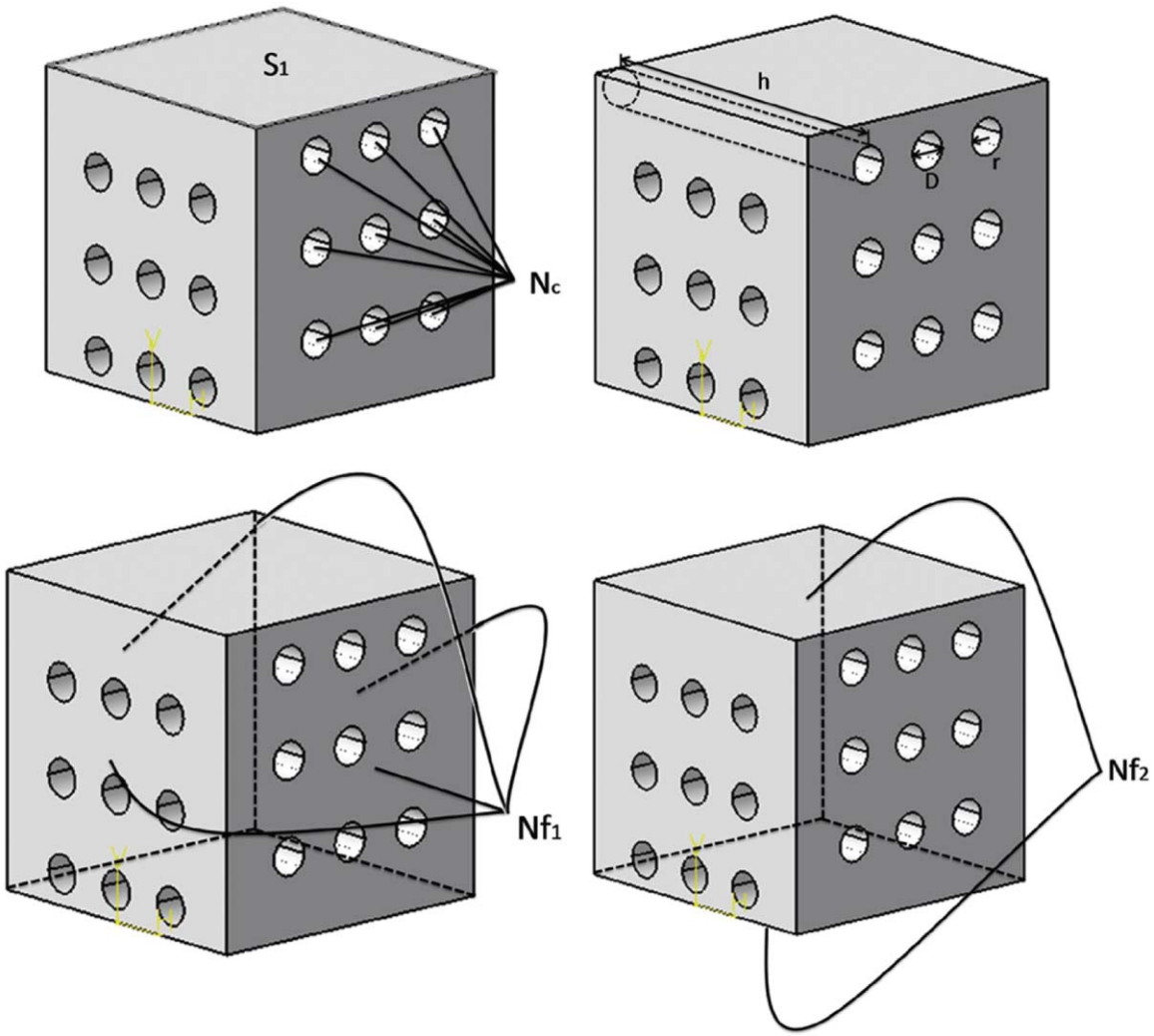

Figure 7. Illustration to explain parameters for the calculation of apparent surface area. [Color figure can be viewed in the online issue, which is available at wileyonlinelibrary.com.]

Figure 6, for 1 day, the attached cell numbers of the dual-pore scaffolds appeared to be greater than that of the control scaffolds because the dual-pore scaffolds have larger surface areas than the control scaffolds due to the global pores, as depicted in Table I. Surface area of the scaffolds was calculated through following equations. Moreover, apparent surface area is the summation of A_0 and A_r.

$$A_0 = (Nf_1 \times S_1) + \{S_1 - (\pi \times r^2 \times N_c)\} \times Nf_2 \quad (2)$$

$$A_r = D \times \pi \times h \times W_{Nc} \quad (3)$$

where A_0 is apparent outer surface area, Nf_1 is the number of face without holes (global pores), S_1 is the area of single face on the scaffold, r is the radius of a hole (a global pore), N_c is number of holes on a face, Nf_2 is the number of face with holes (global pores), A_r is apparent inner surface area generated by needles, D is the diameter of a hole (a global pore), h is the length of a hole (a global pore), and W_{NC} is total number of hole. Each parameter is illustrated in Figure 7. Actually, the apparent outer surface areas are getting smaller as the diameters of the global pores become larger. The apparent outer surface area of the control scaffolds is 600 mm^3, and the apparent outer surface area of the dual-pore scaffolds with the 1200-μm-diameter global pores is approximately 559 mm^3. However, the apparent surface area, including the inner surface, made with needles is changed to approximately 1238 mm^3 in the case of the 1200-μm-diameter global pores, as shown in Table I. Therefore, for the 1-day result, the largest attached cell number should occur in the dual-pore scaffolds with 1200-μm-diameter global pores. However, in our examination, the largest attached cell number was observed in the 820-μm-diameter case. This result could be hypothetically explained as follows: in the case of the 1200-μm-diameter scaffold, cells can easily pass through the global pores because the pore-size is too large before cell attachment to the inner surface. After 7 days, the cell proliferation on the dual-pore scaffolds with 820-μm-diameter global pores appeared to be dramatically greater than those of the control scaffolds and the dual-pore scaffolds with 500- or 1200-μm-diameter global pores. This result seems to be derived from the initial difference in attached cell numbers. However, after 14 days, the cell proliferation of the dual-pore scaffolds with 1200-μm-diameter global pores rapidly increased because sufficient oxygen and nutrients were provided to cells, and cells can easily infiltrate the scaffold. This could be explained by the fact that the interval region between global pores, which is the black solid box in Figure 3, decreased as the global pores increased. In contrast, the cell number in the control scaffolds without global pores was decreased because oxygen and nutrients were undersupplied to cells in a scaffold.

As the reason of cell-proliferation increase, the hypothesis, which global pores act like channel to exchange oxygen, nutrient, and waste, could be accepted clearly via argument about porosity and surface area. As shown in Figure 4, the porosity of SLUP scaffold (global pore = 1200 μm) is larger than that of control scaffold with only 15%. However, as shown in Figure 6, the cell proliferation of SLUP scaffold (global pore = 1200 μm) is dramatically larger than that of control scaffold. It means that the increase of porosity is not the key effect of cell proliferation. Also, at the viewpoint of surface area as depicted in Table I, "apparent surface area" of 1200-μm-macropores scaffold is about two times larger than that of control scaffold. It means that the surface area could be one of the key factors to enhance the cell-proliferation ability of 1200-μm-macropores scaffold. However, the CCK-8 result of 1200-μm-macropores scaffold is almost five times greater than that of control scaffold. Therefore, we could assume that the cell-proliferation in the fabricated SLUP scaffolds with global pores was rapidly increased because global pores act like channels, which are essential for sufficient supply of oxygen and nutrient for cells in the scaffolds.

CONCLUSIONS

In this work, the fabrication method of scaffolds with global/local pores using SLUP technique and needles was proposed. *In vitro* cell examinations were performed using Saos-2 cell to discuss cell proliferation. Porosity and compressive modulus were measured compared with the control scaffold, which is SLUP scaffold without global pores. Moreover, the cell proliferation of SLUP scaffolds with global pores was increased dramatically compared with that of control scaffold, which is SLUP scaffold without global pores. Increasing extent of cell proliferation in the case of SLUP scaffold with global pores could be explained as the result of which the global pores act like channels, which are essential for sufficient supply of oxygen and nutrient for cells in the scaffolds.

ACKNOWLEDGMENTS

This article was supported by Wonkwang University in 2012.

REFERENCES

1. Cancedda, R.; Dozin, B.; Giannoni, P.; Quarto R. *Matrix Biol.* **2003**, *22*, 81.
2. Hollister, S. J.; Maddox, R. D.; Taboas, J. M. *Biomaterials* **2002**, *23*, 4095.
3. Holy, C. E.; Shoichet, M. S.; Davies, J. E. *J. Biomed. Mater. Res. Part A* **2000**, *51*, 376.
4. Nam, Y. S.; Yoon J. J.; Park, T. G. *J. Biomed. Mater. Res.* **2000**, *53*, 1.
5. Hou, Q.; Grijpma, D. W.; Feijen, J. *Biomaterials* **2003**, *24*, 1937.
6. Oh, S. H.; Kang, S. G.; Kim, E. S.; Cho, S. H.; Lee, J. H. *Biomaterials* **2003**, *24*, 4011.
7. Mikos, A. G.; Thorsen, A. J.; Czerwonka, L. A.; Bao, Y.; Langer, R. *Polymer* **1994**, *35*, 1068.
8. Luong, N. D.; Moon, I. S.; Nam, J. D. *Macromol. Mater. Eng.* **2009**, *294*, 699.
9. Li, H.; Chang, J. *Biomaterials* **2004**, *25*, 5473.
10. Sun, J.; Wu, J.; Li, H.; Chang, J. *Eur. Polym. J.* **2005**, *41*, 2443.
11. Lo, H.; Ponticiello, M. S.; Leong, K. W. *Tissue Eng.* **1995**, *1*, 15.
12. Mooney, D. J.; Baldwin, D. F.; Suh, N. P.; Vacanti, J. P.; Langer, R. *Biomaterials* **1995**, *17*, 1417.

13. Kang, H. W.; Tabata, Y.; Ikada, Y. *Biomaterials* **1999**, *20*, 1339.
14. Hollister, S. *J. Nat. Mater.* **2005**, *4*, 518.
15. Williams, J. M.; Adewunmi, A.; Schek, R. M.; Flanagan, C. L.; Krebsbach, P. H.; Feinberg, S. E.; Hollister, S. J.; Dasb, S. *Biomaterials* **2005**, *26*, 4817.
16. Seitz, H.; Rieder, W.; lrsen, S.; Leukers, B.; Tille, C. *J. Biomed. Mater. Res. Part B* **2005**, *74B*, 782.
17. Zhu, N.; Li, M. G.; Cooper, D.; Chen, X. B. *Biofabrication* **2011**, *3*, 1758.
18. Sachlos, E.; Reis, N.; Ainsley, C.; Derby, B.; Czernuszka, J. T. *Biomaterials* **2003**, *24*, 1487.
19. Park, K.; Jung, H.; Son, J. S.; Park, K. D.; Kim, J. *J. Macromol. Symp.* **2007**, *249*, 145.
20. Cho, Y. S.; Kim, B. S.; You, H. K.; Cho, Y.-S. *Curr. Appl. Phys.* in revision.
21. Oh, S. H.; Kang, S. G.; Lee, J. H. *J. Mater. Sci. Mat. Med.* **2006**, *17*, 131.
22. Makaya, K.; Terada, S.; Ohgo, K.; Asakura, T. *J. Biosci. Bioeng.* **2009**, *108*, 68.
23. Oh, S. H.; Park, S. C.; Kim, H. K.; Koh, Y. J.; Lee, J. H.; Lee, M. C; Lee, J. H. *J. Biomater. Sci. Polym. Ed.* **2011**, *22*, 225.
24. Zhang, X.; Cao, C.; Ma, X.; Li, Y. *J. Mater. Sci. Mater. Med.* **2012**, *126*, 1505.
25. Gupta, B.; Patra, S.; Ray, A. R. *J. Appl. Polym. Sci.* **2012**, *126*, 1505.
26. Sethuraman, V.; Makornkaewkeyoon, K.; Khalf, A.; Madihally, S. V. *J. Appl. Polym. Sci.* **2013**, *130*, 4237.